# CIV102 Project Team 404 Design Report

**Authors:** Mustafa Rana, Jiaming Liu, Mohamed Elsayed

**Course:** CIV102: Structures and Materials

**Teaching Assistant:** Jagteshwar Singh

**Date:** November 24, 2025

# Contents

**1 Introduction** **2**

1.1 Structural Summary . . . . . 2

1.2 Major Design Decisions . . . . . 3

**2 Design Iterations** **4**

2.1 Design 0 . . . . . 4

2.2 Design 1: Decreasing the distance between Webs . . . . . 5

2.3 Design 2: Doubling Top Flange Thickness . . . . . 8

2.4 Design 3: Increasing Number of Webs . . . . . 10

2.5 Design 4: Final Iteration . . . . . 12

**3 Conclusion** **13**

# 1 Introduction

The CIV102 final project consisted of designing a beam bridge out of a given quantity of matboard and allowing a train that imposes 400N of force to pass over it with the bridge remaining intact. Our team's initial observations were extremely optimistic, believing that a material such as matboard would be sturdy enough to build a strong bridge that could carry such weight. However, the primary challenge in this project stemmed from the fact that the quantity of matboard as well as the contact cement used to join pieces together were given in very small quantities—mistakes would be unforgiving as our materials supply was sparse. More specifically, we were given a 813 mm × 1016 mm × 1.27 mm sheet of matboard and two tubes of 35mL contact cement—the primary obstacle with these being the scarcity of glue. Thus, proper due diligence had to take place before beginning the building process, which included a number of calculations and simulations with varying cross section geometries and parameters to make an informed decision on how to proceed with the building process. The design report below outline our final bridge composition, key design decisions, what iterations were tested and why they failed, and a summary of the bridge's expected performance during testing.

## 1.1 Structural Summary

The final iteration of our bridge was a reinforced box-girder cross section. Precise dimensions for each component are as given below

- A 92.54 mm wide, 1.27 mm thick bottom flange, spliced together along 2:3 the length of the bridge (leftmost segment being 840 mm long and the other being 420 mm)
- A 100 mm wide, 2.54 mm thick top flange, spliced together along 1:3 the length of the bridge (leftmost segment being 420 mm long and the other being 840 mm)
- Two 66.19 mm tall, 2.54 mm thick webs,
- Fifteen 56.19 mm tall, 77.46 mm wide, 1.27 mm thick diaphragms

To achieve the 2.54 mm thickness of the top flange, two segments of matboard were glued onto each other—this same methodology was implemented for the webs. The net length of the bridge

was 1260 mm (ensuring a 5 mm overhang from each side of the supports as the total distance of the gap and the width of the supports is 1250 mm), while the total height was 60 mm (inclusive of the thickness of the flange, glue tabs and height of the webs). The total width of the bridge varied as you move downwards, as the top flange is 100 mm wide while the remaining components are 92.54 mm wide—including the gap between the two webs.

## 1.2 Major Design Decisions

1. **Splicing Position**

   As the length of the matboard was insufficient in meeting the 1250 mm requirement, a splice had to be placed somewhere to connect two pieces of matboard to meet the length requirement. From our intuition, we made the decision to place the splice at a point between the middle and the end of the length of the bridge (i.e. 1:3 or 2:3 the length of the bridge). This is simply due to the bending moment being greatest at the middle and shear force being greater at the edges, thus some point in between both would be the ideal location for the splice. This location was alternated in between the top and bottom flanges to ensure that one glaring weakness wasn't generated from the splice being in the same location across the entirety of the bridge.

2. **Locations of Diaphragms**

   We chose to have regions of diaphragms in places with the greatest chance for Case 3 buckling. As the major purpose of the diaphragms was to alleviate the forces from the webs and reduce the chance of web buckling, we placed three diaphragms closely in the middle and evenly spaced the remaining diaphragms out (shown in Fig. 1 below). This ensured that our bridge would have a greater chance of surviving in this certain buckling scenario.

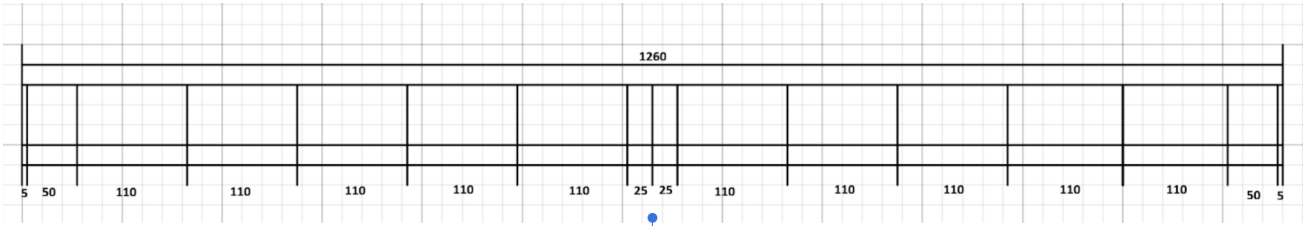



Figure 1: Lengthwise view of the bridge, indicating placements of diaphragms (scale in millimeters)

3. **Selecting a Cross Section**

   To select a cross section, varying iterations of cross sections that stemmed from Design 0 were tested using computation software and code to find out their failure loads and reasons. After 4 iterations of cross sections, a successful cross section was accumulated as a result of all previous tests, which ended up successfully passing load case one.

# 2 Design Iterations

This segment of the report will highlight the order in which the overall design of the bridge was iterated to achieve our final product. Justification and evidence for each iteration is provided in the form of code and computations.

## 2.1 Design 0

Design 0 was provided as a base-case for what a possible design for the bridge could look like. To understand where the bridge would fail and how, the bridge's properties were analyzed and calculated to be the following (A 3-D live model was generated to better visualize the region of failure, shown in Fig. 2):

- $I \approx 418 \times 10^3\,\text{mm}^4$,
- $Q \approx 6.2 \times 10^3\,\text{mm}^3$
- $Q_{\text{glue}} \approx 4.4 \times 10^3\,\text{mm}^3$
- $y_{\text{bar}} \approx 41.4\,\text{mm}$.
- Flexural compression FOS = 1.042,
- Lowest Shear FOS = 2.678.
- Top Flange Buckling FOS = 0.64.
- Minimum FOS $\approx$ 0.64
- Predicted Fail Load = 256 N.

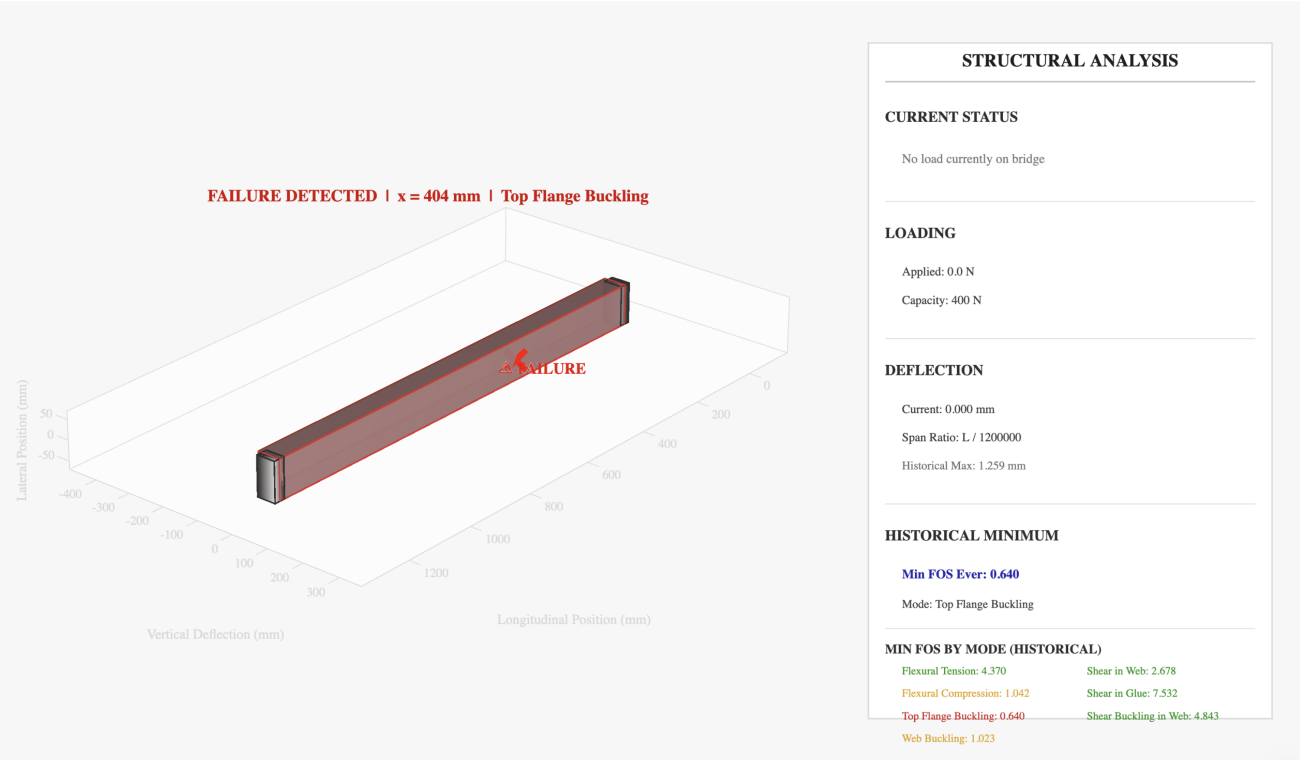



Figure 2: 3D simulation of Design 0 undergoing Load Case 1 using MATLAB

The computations clearly showed that the bridge would fail by top flange buckling between the webs. Thus, the short term goal now was to combat this flaw and increase flange stability and resistance-to-bending.

## 2.2 Design 1: Decreasing the distance between Webs

As the top flange was buckling in design 0, a possible iteration to combat this issue was to decrease the spacing between the two webs of the design. This would require the webs to be cut out from the bottom flange as well and reconnected with more glue tabs—a low-fidelity diagram is shown in Fig. 3.

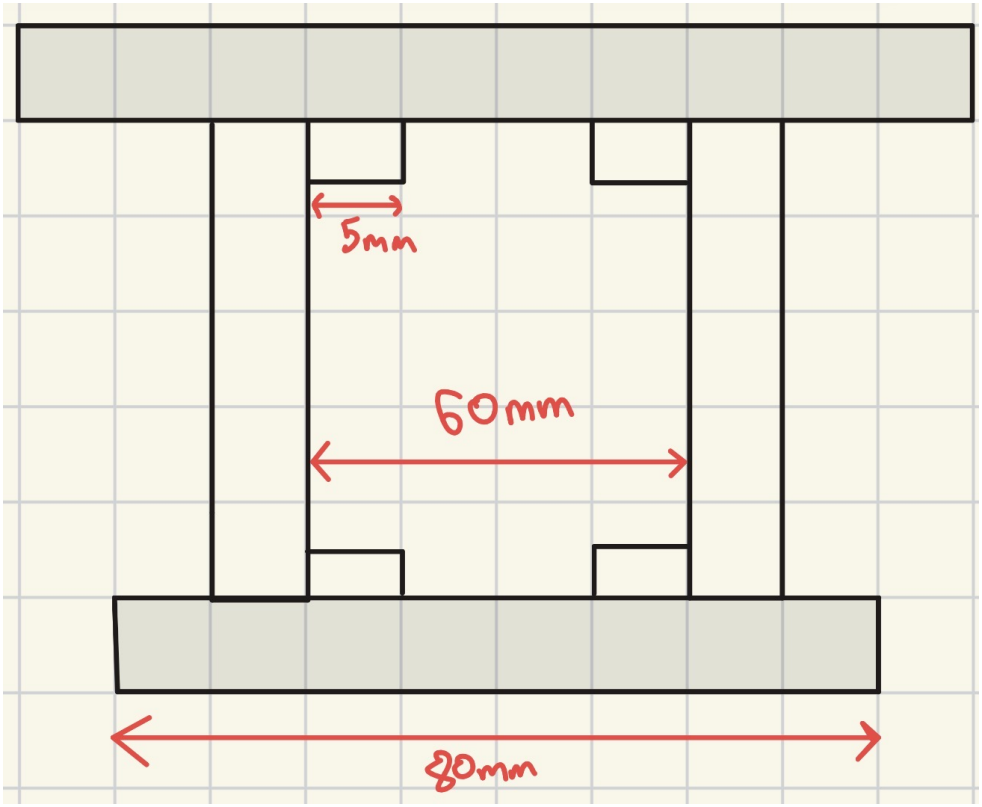



Figure 3: First iteration cross section of the bridge, with decreased spacing between webs to reduce chances of top flange buckling (all properties not listed are the same as Design 0)

By adjusting the distance between the two webs, we attempted to mitigate failure due to top flange buckling. The justification for this is given by the following equation:

$$\sigma_{cr} = k \frac{\pi^2 E}{12(1-\nu^2)} \left(\frac{t}{b}\right)^2 \tag{1}$$

where $b$ provides the clear width between the webs. By decreasing this space, the critical value for stress at the top flange increases and increasing it's minimum FOS. Another computation was run with the new cross section and the results were provided in Fig. 4:

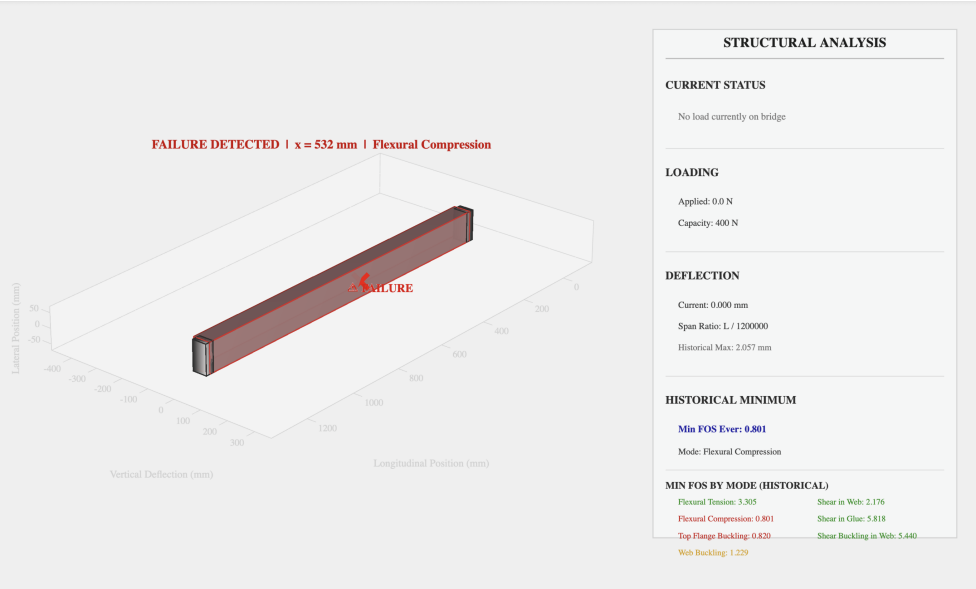



Figure 4: 3D simulation of Design 1 undergoing Load Case 1 using MATLAB

Observing the new results showed the following factors of safety:

- Flexural compression FOS = 0.801,
- Lowest Shear FOS = 2.176.
- Top Flange Buckling FOS = 0.82.
- Web Buckling FOS = 1.229.
- Flexural Tension FOS = 3.305.
- Minimum FOS $\approx$ 0.801
- Predicted Fail Load = 321 N.

The new iteration shows weakness in flexural compression, with a factor of safety of 0.801, thus the bridge would still fail to Load Case 1. The next iteration would have to combat flexural compression.

## 2.3 Design 2: Doubling Top Flange Thickness

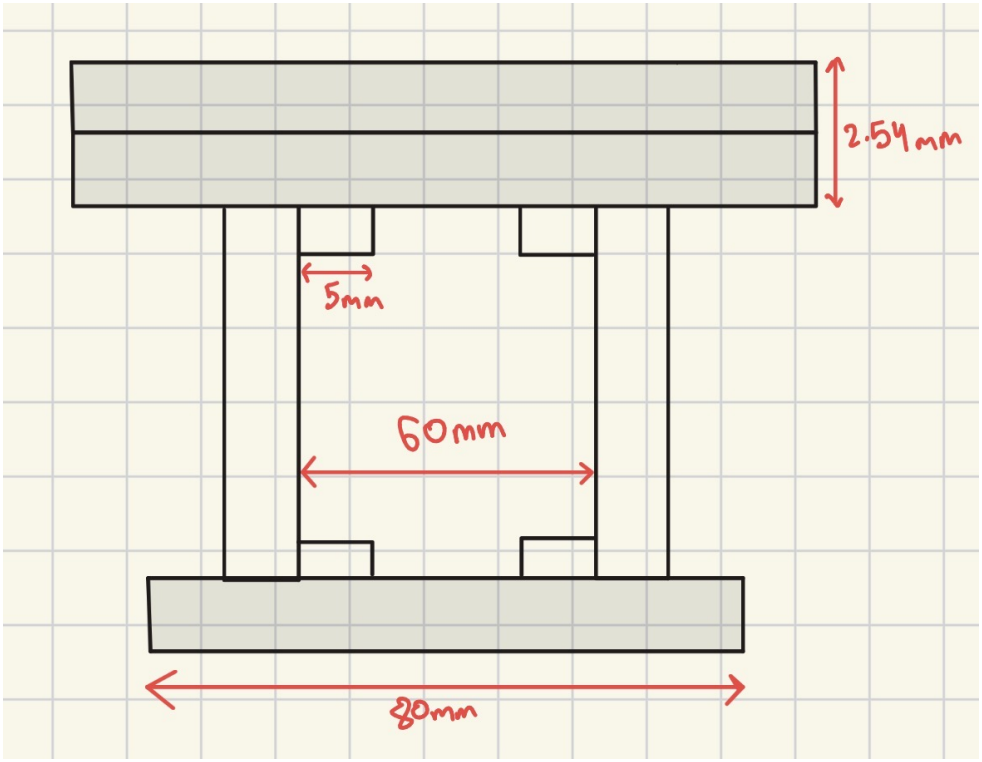



Figure 5: Second iteration cross section of the bridge, with doubled top flange thickness (all properties not listed are the same as Design 0)

Our next iteration was to double the top flange thickness. Doubling the thickness of the top flange increases the section modulus about the major bending axis, thereby reducing the compressive bending stress in the flange. The bending stress at the top fibre is

$$\sigma_{\text{top}} = \frac{M y_{\text{top}}}{I} = \frac{M}{S_{\text{top}}}, \tag{2}$$

where $S_{\text{top}} = I/y_{\text{top}}$ is the top–fibre section modulus. When an additional layer of thickness $\Delta t$ is laminated to the top flange, the added area is located far from the neutral axis, producing an increase in second moment of area given approximately by

$$I_{\text{new}} = I_{\text{old}} + A_{\text{add}}\, d^2, \tag{3}$$

where $d$ is the vertical distance from the old neutral axis to the added layer. Because this added material lies near the extreme fibre, $I_{\text{new}} > I_{\text{old}}$. Therefore, doubling the top–flange thickness decreases the flexural compressive stress and significantly increases the flange's resistance to local

buckling. With this in mind, another simulation was ran on the new set of values and is shown in Fig. 6:

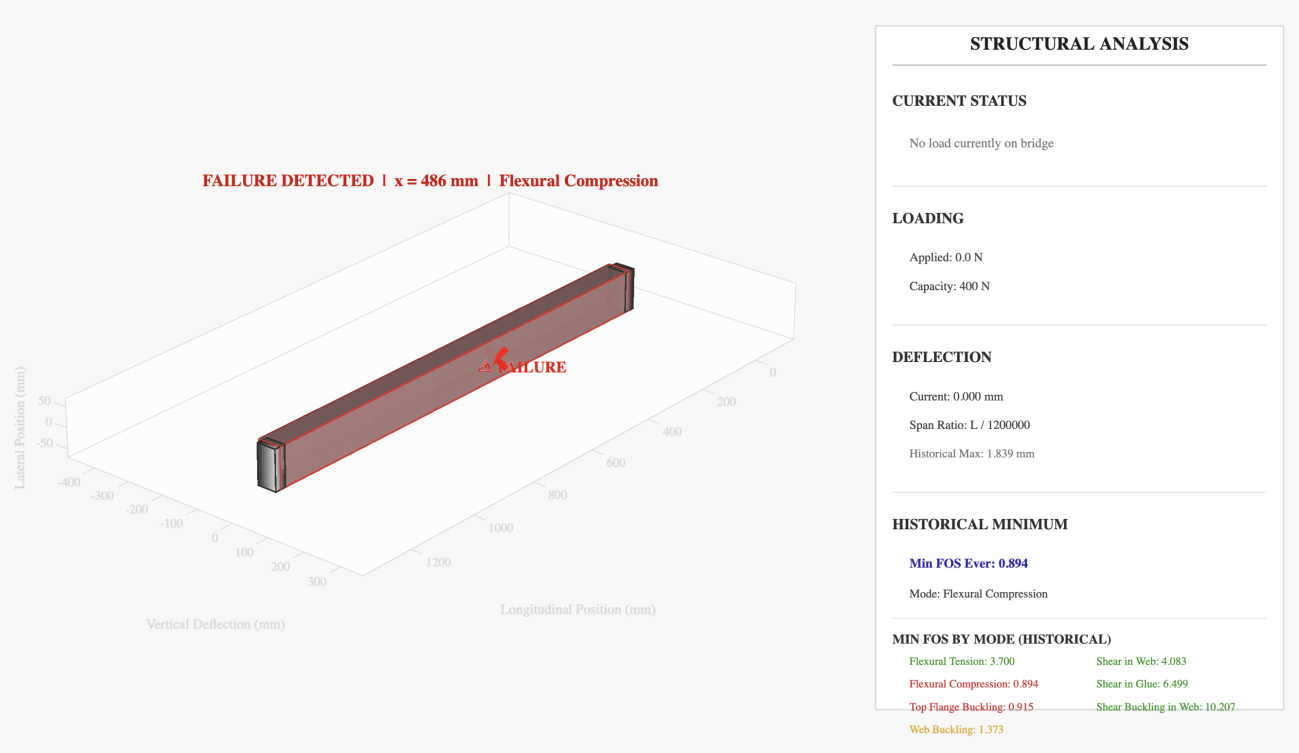



Figure 6: 3D simulation of Design 2 undergoing Load Case 1 using MATLAB

The new factors of safety are as follows:

- Flexural compression FOS = 0.894,
- Lowest Shear FOS = 4.083.
- Top Flange Buckling FOS = 0.915.
- Web Buckling FOS = 1.373.
- Flexural Tension FOS = 3.700.
- Minimum FOS $\approx$ 0.894
- Predicted Fail Load = 358 N.

Although the goal to increase resistance to flexural compression was achieved, the cross section still failed to flexural compression, highlighting the need to further combat this issue.

## 2.4 Design 3: Increasing Number of Webs

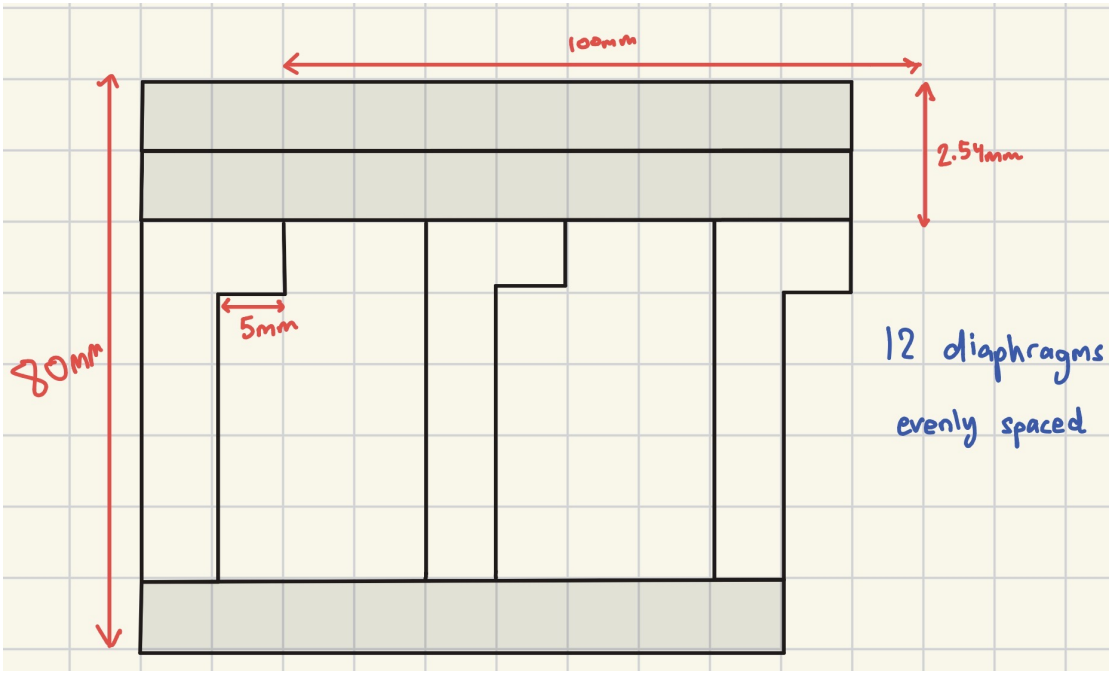



Figure 7: Third iteration cross section of the bridge, implemented with 3 webs to decrease risk of flexural compression

Another possible iteration to combat flexural compression was to add another web. To do so, the height of the cross section had to be adjusted. By adding another web, this new cross section attempts to solve the top flexural issue in the same way as iteration one did—by decreasing the effective area between two webs and adding more support underneath the top flange in order to decrease the value of $b$ in Eq. 1 and subsequently increase resistance to flexural compression. Doing so provided the following simulation:

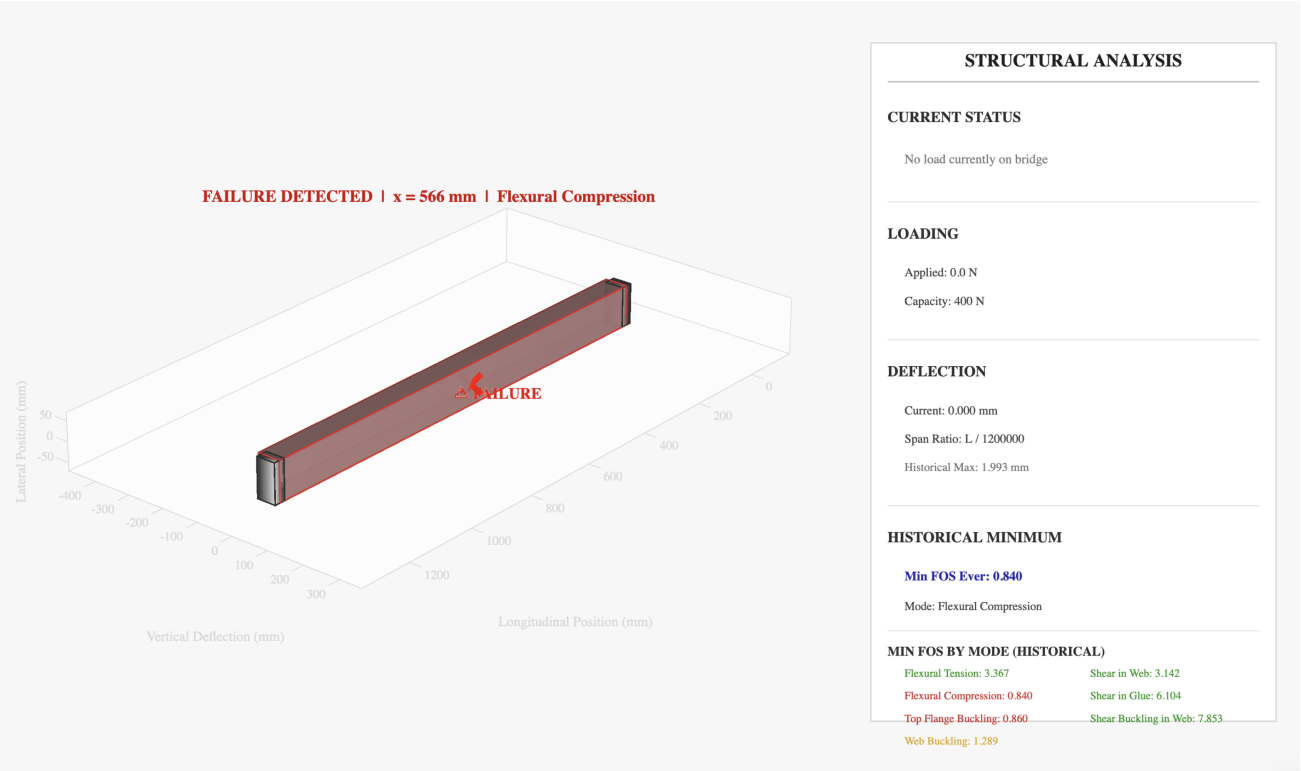



Figure 8: 3D simulation of Design 3 undergoing Load Case 1 using MATLAB

The new factors of safety are as follows:

- Flexural compression FOS = 0.840,
- Lowest Shear FOS = 3.142.
- Top Flange Buckling FOS = 0.86.
- Web Buckling FOS = 1.289.
- Flexural Tension FOS = 3.367.
- Minimum FOS $\approx$ 0.840
- Predicted Fail Load = 336 N.

This iteration proved to be a mistake as practically all factors of safety decreased and the predicted fail load decreased by 22N. This decrease in performance was attributed to the increased height of the cross section, which ulimtately caused too overwhelming of a change in the centroidal axis, buckling, and moment of inertia, hence causing a net decrease in compressive resistance even though another web was added.

## 2.5 Design 4: Final Iteration

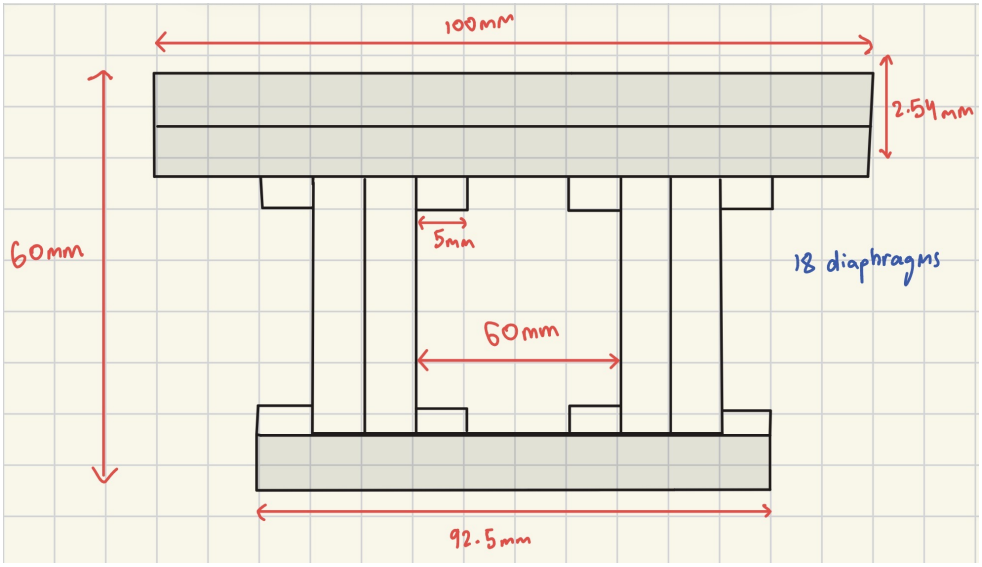



Figure 9: Final iteration cross section of the bridge, with shortened height, increased bottom flange width and 4 webs

As increasing the height clearly showed a decrease in resistance to the train's forces, another approach was taken to increase the number of webs. Two webs were placed back-to-back on each pre-existing web, while the height was decreased to 60 mm instead of the previous 80. Moreover, the width of the bottom flange was adjusted to better maximize the use of the matboard, providing the following cross section shown above in Fig. 9. Running a simulation on this cross section provided the following results:

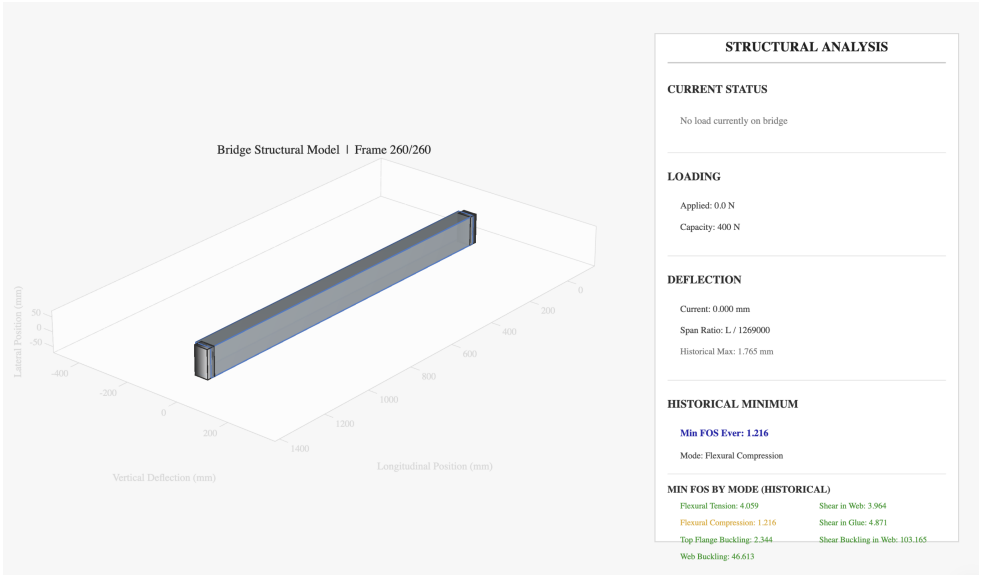



Figure 10: 3D simulation of Design 0 undergoing Load Case 1 using MATLAB

The new factors of safety are as follows:

- Flexural compression FOS = 1.216,
- Lowest Shear FOS = 3.964.
- Top Flange Buckling FOS = 2.344.
- Web Buckling FOS = 46.613.
- Flexural Tension FOS = 4.059.
- Minimum FOS $\approx$ 1.216
- Predicted Fail Load = 487 N.

This finalized cross section showed a phenomenal increase in resistance to the train's applied forces. With this iteration, the lowest FOS (compressive forces) had crossed 1.000, highlighting that the cross section survived Load Case 1. Moreover, the FOS for web buckling had increased a tremendous amount, showing that doubling the webs back-to-back greatly improves resistance to Case 3 Buckling. Thus, this cross section was the finalized choice for production.

# 3 Conclusion

When optimising a matboard bridge under stringent material constraints, data-driven decision making is crucial, as this project's iterative design process showed. Every iteration after Design 0 focused on a structural weakness that was readily apparent. While Design 2 improved flexural compression resistance by doubling the top-flange thickness, Design 1 greatly increased the flange's local buckling capacity by reducing the web spacing. However, Design 3 was a step in the wrong direction and decreased the cross-sections resistance to forces. The development of Design 4, which successfully combined paired webs, controlled section height, and optimised flange dimensions, was influenced by this setback and greatly improved upon all previous designs.

All pertinent safety factors were significantly increased in the final design (Design 4), with the predicted fail load increasing from 256N to 487N and the minimum FOS increasing from 0.64 in the baseline design to 1.216. These enhancements show that theoretical calculations, simulation outcomes, and realistic fabrication constraints are successfully aligned. In the end, the completed

cross section not only met the requirement of withstanding the 400N train load, but it also did so with a structurally sound configuration and effective material use. In structural engineering design, this procedure emphasises the importance of focused iteration, analytical justification, and cautious material management.